

## Effect of CaO content in raw material on the mineral composition of ferric-rich sulfoaluminate clinker

Yao, Xingliang; Yang, Shizhao; Dong, Hua; Wu, Shuang; Liang, Xuhui; Wang, Wenlong

**DOI**

[10.1016/j.conbuildmat.2020.120431](https://doi.org/10.1016/j.conbuildmat.2020.120431)

**Publication date**

2020

**Document Version**

Final published version

**Published in**

Construction and Building Materials

**Citation (APA)**

Yao, X., Yang, S., Dong, H., Wu, S., Liang, X., & Wang, W. (2020). Effect of CaO content in raw material on the mineral composition of ferric-rich sulfoaluminate clinker. *Construction and Building Materials*, 263, Article 120431. <https://doi.org/10.1016/j.conbuildmat.2020.120431>

**Important note**

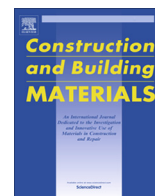
To cite this publication, please use the final published version (if applicable). Please check the document version above.

**Copyright**

Other than for strictly personal use, it is not permitted to download, forward or distribute the text or part of it, without the consent of the author(s) and/or copyright holder(s), unless the work is under an open content license such as Creative Commons.

**Takedown policy**

Please contact us and provide details if you believe this document breaches copyrights. We will remove access to the work immediately and investigate your claim.



# Effect of CaO content in raw material on the mineral composition of ferric-rich sulfoaluminate clinker

Xingliang Yao<sup>a,b</sup>, Shizhao Yang<sup>a</sup>, Hua Dong<sup>b</sup>, Shuang Wu<sup>a</sup>, Xuhui Liang<sup>b</sup>, Wenlong Wang<sup>a,\*</sup>

<sup>a</sup> National Engineering Laboratory for Reducing Emissions from Coal Combustion, Engineering Research Center of Environmental Thermal Technology of Ministry of Education, Shandong Key Laboratory of Energy Carbon Reduction and Resource Utilization, School of Energy and Power Engineering, Shandong University, Jinan, Shandong 250061, China

<sup>b</sup> Microlab, Faculty of Civil Engineering and Geosciences, Delft University of Technology, 2628 CN Delft, The Netherlands

## HIGHLIGHTS

- CaO content in raw materials influences the phase composition of the FR-CSA clinker.
- Lower CaO content in raw mixture promotes the incorporation of Fe<sub>2</sub>O<sub>3</sub> into ye'elimite.
- A method to optimize the phase composition of FR-CSA clinker is provided.

## ARTICLE INFO

### Article history:

Received 18 March 2020  
Received in revised form 28 July 2020  
Accepted 30 July 2020

### Keywords:

Ferric-rich sulfoaluminate cement  
CaO  
Phase composition  
Iron-bearing phase

## ABSTRACT

Ferric-rich calcium sulfoaluminate (FR-CSA) cement is an eco-friendly cement. Fe<sub>2</sub>O<sub>3</sub> exists in different minerals of FR-CSA clinker, e.g., Ca<sub>4</sub>Al<sub>2</sub>Fe<sub>2</sub>O<sub>10</sub> (C<sub>4</sub>AF), Ca<sub>2</sub>Fe<sub>2</sub>O<sub>5</sub> (C<sub>2</sub>F), and Ca<sub>4</sub>Al<sub>6-2x</sub>Fe<sub>2x</sub>SO<sub>16</sub> (C<sub>4</sub>A<sub>3-x</sub>F<sub>x</sub>S̄). The mineral composition depends on the chemical composition of the raw materials and significantly determines the reactivity of FR-CSA cement. To optimize the phase composition of the FR-CSA clinker, chemical reagent raw mixtures with different amounts of CaO were used to prepare the FR-CSA clinker. X-ray diffraction (XRD) analysis, Rietveld quantitative phase analysis (RQPA), Fourier Transform Infrared spectroscopy (FT-IR), and scanning electron microscopy/energy-dispersive spectroscopy (SEM/EDS) were used to identify the mineralogical conditions of the FR-CSA clinker. The results indicated that the amounts of CaO in raw materials greatly affected the iron-bearing phase formation in the FR-CSA clinker. With decreasing CaO content involved in calcination reaction, the amounts of Fe<sub>2</sub>O<sub>3</sub> incorporated in C<sub>4</sub>A<sub>3-x</sub>F<sub>x</sub>S̄ increased up to 17.72 wt% (where  $x = 0.36$ ). The findings make it possible to optimize the mineral composition of the FR-CSA clinker by changing the CaO content in raw materials. Furthermore, low CaO content in the raw material is beneficial to the formation of C<sub>4</sub>A<sub>3-x</sub>F<sub>x</sub>S̄, which enables the use of solid wastes containing low calcium for producing FR-CSA cement.

© 2020 Elsevier Ltd. All rights reserved.

## 1. Introduction

Calcium sulfoaluminate (CSA) cement is a new type of cement first developed in China 40 years ago. It exhibits some great performances, such as high early strength, rapid setting, and shrinkage-compensating, et al. for certain applications [1–3]. The major phases of CSA clinker are ye'elimite (Ca<sub>4</sub>Al<sub>6</sub>SO<sub>16</sub>, C<sub>4</sub>A<sub>3</sub>S̄), belite (Ca<sub>2</sub>SiO<sub>4</sub>, C<sub>2</sub>S), and the minor phases are anhydrite (CaSO<sub>4</sub>, C̄S), brownmillerite (Ca<sub>4</sub>Al<sub>2</sub>Fe<sub>2</sub>O<sub>10</sub>, C<sub>4</sub>AF), and Ca<sub>2</sub>Fe<sub>2</sub>O<sub>5</sub> (C<sub>2</sub>F), et al. [4,5]. C<sub>4</sub>A<sub>3</sub>S̄ in CSA contains smaller amount of CaO than the alite

(Ca<sub>3</sub>SiO<sub>5</sub>, C<sub>3</sub>S) in Portland cement (PC). Therefore, the production of CSA clinker requires lower amount of limestone consumption compared with Portland cement (PC) production, and reduces the CO<sub>2</sub> emission [6]. Meanwhile, the preparation temperature of CSA clinker ranges from 1200 to 1300 °C, which is 200 °C lower than the calcination temperature of Portland cement clinker, reducing energy consumption during the calcination process [7,8]. Besides, the CSA clinkers are easier to grind due to their high porosity, which further reduces energy consumption during the grinding process. Therefore, the characters of energy-saving, low CO<sub>2</sub> emission, and good mechanical performance, make CSA cement as an ideal alternative to PC in certain applications.

However, the utilization of CSA cement is still limited. The main obstacle to the application of CSA cement on a massive scale is its

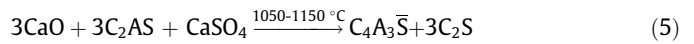
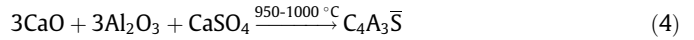
\* Corresponding author.

E-mail addresses: [yaoxl1991@163.com](mailto:yaoxl1991@163.com) (X. Yao), [H.Dong@tudelft.nl](mailto:H.Dong@tudelft.nl) (H. Dong), [wwenlong@sdu.edu.cn](mailto:wwenlong@sdu.edu.cn) (W. Wang).

high cost of raw materials, which requires expensive natural bauxite. Therefore, the consumption of bauxite, which contains high amount of  $\text{Al}_2\text{O}_3$ , should be minimized.  $\text{Fe}_2\text{O}_3$  is usually used as an alternative component to  $\text{Al}_2\text{O}_3$  during the production process of CSA clinker, resulting in the FR-CSA cement. Note that the required amount of  $\text{Fe}_2\text{O}_3$  in the FR-CSA clinker ranges from 5 to 13 wt%, while only 1 to 3 wt% of  $\text{Fe}_2\text{O}_3$  exist in the CSA clinker [9]. In addition to  $\text{C}_2\text{F}$  and  $\text{C}_4\text{AF}$ , the  $\text{Fe}_2\text{O}_3$  can also be incorporated in  $\text{C}_4\text{A}_3\bar{\text{S}}$  to form  $\text{C}_4\text{A}_{3-x}\text{F}_x\bar{\text{S}}$  in the FR-CSA clinker, where the value of  $x$  represents the amount of  $\text{Fe}_2\text{O}_3$  incorporated in  $\text{C}_4\text{A}_3\bar{\text{S}}$  [10,11]. Similar to the reaction of  $\text{C}_4\text{A}_3\bar{\text{S}}$  with water,  $\text{C}_4\text{A}_{3-x}\text{F}_x\bar{\text{S}}$  can react with water and form ettringite, which is conducive to the development of compressive strength [9]. Thus,  $\text{Fe}_2\text{O}_3$  can be used as a partial replacement of  $\text{Al}_2\text{O}_3$  to reduce the consumption of aluminum source. With the reduced requirement of the consumption of aluminum source, some aluminum-bearing solid wastes or low-grade  $\text{Al}_2\text{O}_3$  minerals can be used, and the cost of FR-CSA cement can be reduced.

During the calcination process of the FR-CSA clinker, the distributions of  $\text{Fe}_2\text{O}_3$  in iron-bearing phases are affected by the chemical composition of the raw material. And the iron-bearing phase composition influences the mechanical properties of the FR-CSA cement [12,13]. To optimize the iron-bearing phase composition of FR-CSA clinker, it is important to know the effect of raw material composition on the iron-bearing phase formation in the FR-CSA clinker. Many researchers have investigated the effect of raw material on the phase composition of the FR-CSA clinker. Y. Huang et al. concluded that the addition of  $\text{Fe}_2\text{O}_3$  could promote higher  $\text{Fe}_2\text{O}_3$  incorporation into CSA clinker, forming  $\text{C}_4\text{A}_{2.7}\text{F}_{0.3}\bar{\text{S}}$  [14]. Dun Chen et al. studied the effect of  $\text{Fe}_2\text{O}_3$  content on the incorporation level of  $\text{Fe}_2\text{O}_3$  into  $\text{C}_4\text{A}_{3-x}\text{F}_x\bar{\text{S}}$  and concluded that 22.31 wt%  $\text{Fe}_2\text{O}_3$  reached maximum incorporation content into  $\text{C}_4\text{A}_{3-x}\text{F}_x\bar{\text{S}}$  [10]. Idrissi M. et al. identified the mineralogical conditions of iron inclusion during the formation of  $\text{C}_4\text{A}_3\bar{\text{S}}$  made from different raw materials. The maximum fraction of  $\text{Fe}_2\text{O}_3$  in the  $\text{C}_4\text{A}_3\bar{\text{S}}$  was 21.5 wt% [15]. Bruno Touzo et al. studied the phase equilibria in the  $\text{CaO}-\text{Al}_2\text{O}_3-\text{Fe}_2\text{O}_3-\text{SO}_3$  system at 1325 °C and got that the value of  $x$  increased to a plateau of 0.34 [16]. All the aforementioned researches were focused on the effect of  $\text{Fe}_2\text{O}_3/(\text{Fe}_2\text{O}_3 + \text{Al}_2\text{O}_3)$  ratio in  $\text{CaO}-\text{Al}_2\text{O}_3-\text{Fe}_2\text{O}_3-\text{SO}_3$  system. However, CaO is a primary content in the FR-CSA clinker. During the calcination of FR-CSA clinker, CaO almost participates in all the phase formation reactions and distributes in all minerals according to Eqs. (1)–(8) [17]. Thus, CaO content is a critical parameter for the phase composition in FR-CSA clinker.

Bruno Touzo et al. also put forward that  $\text{Fe}_2\text{O}_3/(\text{Fe}_2\text{O}_3 + \text{Al}_2\text{O}_3)$  was not the only parameter influencing the value of  $x$ . The CaO content and the content of other elements would shift the equilibrium of the reactions during calcination. C. Ren et al. and Y. Shen et al. prepared the CSA clinker from solid wastes and demonstrated that the CaO or  $\text{CaSO}_4$  content affected the formation of  $\text{C}_2\text{AS}$  and  $\text{C}_4\text{A}_3\bar{\text{S}}$  in CSA clinker [18,19]. However, all the researches were about the effect of CaO content on phase formation or  $\text{C}_4\text{A}_3\bar{\text{S}}$  in CSA clinker. Investigation on the effect of CaO content on the formation of iron-bearing phases in FR-CSA clinker is still limited. To optimize the iron-bearing phase composition of the FR-CSA clinker, it is necessary to investigate the effect of CaO content on the iron-bearing phase formation in FR-CSA clinker.



The aim of this work is to investigate the feasibility of optimizing the phase composition of FR-CSA clinker by changing the CaO content in raw materials. In our research, the FR-CSA clinkers were prepared from chemical reagents, in which different amount of  $\text{Ca}(\text{OH})_2$  and  $\text{CaSO}_4$  were added to change the CaO content, respectively. X-ray diffraction (XRD) analysis, Rietveld quantitative phase analyses (RQPA), and Fourier Transform Infrared spectroscopy (FT-IR) were used to identify and quantify the phase composition, respectively. Scanning electron microscopy/energy-dispersive spectroscopy (SEM/EDS) was used to detect the distribution of  $\text{Fe}_2\text{O}_3$  in iron-bearing phases. Along with the variation of iron-bearing phase compositions, the incorporated content of  $\text{Fe}_2\text{O}_3$  in  $\text{C}_4\text{A}_{3-x}\text{F}_x\bar{\text{S}}$  was calculated. The effective utilizations of  $\text{Fe}_2\text{O}_3$  and  $\text{Al}_2\text{O}_3$  in the FR-CSA clinker were also calculated according to the distribution of  $\text{Fe}_2\text{O}_3$  and  $\text{Al}_2\text{O}_3$  in different phases. Finally, the clinkers with different  $\text{C}_4\text{AF}$  designed and with different calcination process were also got to certify the effect of CaO content in raw materials.

## 2. Experiment

### 2.1. Preparation of FR-CSA clinker

#### 2.1.1. Raw materials

The chemical pure reagents ( $\text{Ca}(\text{OH})_2$ ,  $\text{Al}_2\text{O}_3$ ,  $\text{CaSO}_4$ ,  $\text{Fe}_2\text{O}_3$ , and  $\text{SiO}_2$ ), which were supplied by Sinopharm Group Chemical Reagent Co., Ltd., Shanghai, China, were used as raw materials to prepare the FR-CSA clinker. Among them,  $\text{Ca}(\text{OH})_2$  was used as the source of CaO.  $\text{CaSO}_4$  was not only used as the source of CaO but also was the source of  $\text{SO}_3$  during the calcination process of the FR-CSA clinker.

The FR-CSA clinker was synthesized from chemical reagent raw materials based on stoichiometric amount. The ratios of raw materials were calculated according to the Bogue method, which was adapted for CSA clinker by assuming phase assemblage of  $\text{C}_2\text{S}$ ,  $\text{C}_4\text{A}_3\bar{\text{S}}$ ,  $\text{C}_4\text{AF}$ , and  $\text{CaSO}_4$  as given in Eqs. (9)–(12) [20]:

$$\text{C}_4\text{AF}\% = (\text{F}\%) \times \left( \frac{M_{\text{C}_4\text{AF}}}{M_{\text{F}}} \right) \quad (9)$$

$$\text{C}_2\text{S}\% = (\text{S}\%) \times \left( \frac{M_{\text{C}_2\text{S}}}{M_{\text{S}}} \right) \quad (10)$$

$$\text{C}_4\text{A}_3\bar{\text{S}}\% = \left( \text{A}\% - \text{C}_4\text{AF}\% \times \frac{M_{\text{A}}}{M_{\text{C}_4\text{AF}}} \right) \times \frac{M_{\text{C}_4\text{A}_3\bar{\text{S}}}}{3 \times M_{\text{A}}} \quad (11)$$

$$\text{C}\bar{\text{S}}\% = \left( \bar{\text{S}}\% - \text{C}_4\text{A}_3\bar{\text{S}}\% \times \frac{M_{\bar{\text{S}}}}{M_{\text{C}_4\text{A}_3\bar{\text{S}}}} \right) \times \frac{M_{\text{C}\bar{\text{S}}}}{M_{\bar{\text{S}}}} \quad (12)$$

The CaO content in the FR-CSA clinkers was termed as the alkalinity modulus ( $C_m$ ) and defined using Eq. (13) [9]. The value of  $x$  indicates the degree to which CaO in the raw material satisfies the reaction with  $\text{SiO}_2$ ,  $\text{Al}_2\text{O}_3$ , and  $\text{Fe}_2\text{O}_3$  to form useful minerals

(i.e.,  $C_4A_3\bar{S}$ ,  $C_4AF$ , and  $C_2S$ ) in the CSA clinker. It is usually lower than 1.00 to avoid the existence of free calcium oxide (f-CaO) in the CSA clinker. The  $C_m$  is calculated as follows.

$$C_m = \frac{\text{CaO} - 0.7\text{TiO}_2}{1.87\text{SiO}_2 + 0.73(\text{Al}_2\text{O}_3 - 0.64\text{Fe}_2\text{O}_3) + 1.40\text{Fe}_2\text{O}_3} \quad (13)$$

According to Table 1 and Eqs. (9)–(12), five FR-CSA clinkers with different CaO content were designed and termed as  $C_{0.90}$ ,  $C_{0.95}$ ,  $C_{1.00}$ ,  $C_{1.05}$ , and  $C_{1.10}$ , corresponding to the  $C_m$  values of 0.90, 0.95, 1.00, 1.05, and 1.10, respectively. The targeted phase ratio of  $C_4A_3\bar{S}$ : $C_4AF$ : $C_2S$ : $\text{CaSO}_4$  was 40%:20%:30%:10% by mass. Furthermore, to verify the results from the above raw mixture, as shown in Table 2, another raw mixture that targeted phase ratio of  $C_4A_3\bar{S}$ : $C_4AF$ : $C_2S$ : $\text{CaSO}_4$  was 30%:30%:30%:10% by mass was also designed and termed as  $C_{0.90-1}$ ,  $C_{0.95-1}$ ,  $C_{1.00-1}$ ,  $C_{1.05-1}$ , and  $C_{1.10-1}$ .

In addition, CaO exists in the form of  $\text{Ca}(\text{OH})_2$  and  $\text{CaSO}_4$ . The decomposition temperature of  $\text{Ca}(\text{OH})_2$  is below 900 °C, which is lower than the formation temperature of  $C_4A_3\bar{S}$ ,  $C_2S$ ,  $C_4AF$ , and  $C_2AS$ . However, the decomposition temperature of  $\text{CaSO}_4$  is higher than 1170 °C. Thus, the amount of  $\text{CaSO}_4$  further affects the formation of minerals in FR-CSA clinker, which is not the same as the effect of CaO content. To explore the effect of CaO in the form of  $\text{CaSO}_4$  on the phase formation of FR-CSA clinker, as shown in Table 2, another five clinkers with different  $\text{CaSO}_4$  contents but same  $C_m$ , termed as  $S_0$ ,  $S_5$ ,  $S_{10}$ ,  $S_{15}$ , and  $S_{20}$ , were designed. The extra content of  $\text{CaSO}_4$  was 0, 5, 10, 15, and 20 wt% in FR-CSA clinkers, respectively. The value of  $C_m$  was 1.00 and  $\text{Al}_2\text{O}_3/\text{Fe}_2\text{O}_3$  ratios were same for all the clinkers.

### 2.1.2. Preparation process

The raw materials were dried at  $105 \pm 5$  °C until constant weight. Next, raw materials with a certain ratio were ground and sieved through a 200-mesh sieve to obtain the desired raw mixture. Then the raw mixture was calcined at 1250 °C for 30 min, and rapidly cooled at 20 °C to obtain FR-CSA clinkers. Finally, it was ground and sieved through a 200-mesh sieve for the following analyses.

### 2.2. Characterization methods

The f-CaO content in the FR-CSA clinkers was determined by the phenyl formic acid titration method in accordance with the Chinese standard GB/T 176-2017 [21].

The mineral composition of different clinkers was identified using an X-ray diffractometer (Aeris, MalvernPanalytical, Netherlands) with Cu-K $\alpha$  radiation at 40 kV and 15 mA. The measurement time was 0.5 h per pattern with a scanning speed of 0.6°/min during the  $2\theta$  range of 10–50° for qualitative analysis. RQPA was applied to perform a quantitative phase analysis using X'Pert

HighScore Plus software. The crystallographic structures of phases involved in RQPA were listed in Table 3. Except for  $C_4A_{3-x}F_x\bar{S}$ , which was described using a refined crystallographic structure, other minerals remained the same with the reference phases. The refinement parameters were in order as follows: emission profile, background coefficients, instrument parameters, zero error, Lorentz polarization factor, unit cell parameters and preferred orientation coefficient.

The FT-IR spectra of the FR-CSA clinkers were obtained using a Nicolet iS (Thermo Fisher, USA). For the analysis of the different FR-CSA clinkers, 2 mg powder samples were obtained by grinding the clinker in 400 mg of KBr. FT-IR scans were performed at frequencies from 400  $\text{cm}^{-1}$  to 1200  $\text{cm}^{-1}$  with a resolution of 4  $\text{cm}^{-1}$  at 20 °C. The results were analyzed using OMNIC software.

SEM (JSM-IT500HR, JEOL, Japan) with the 5 kV accelerated voltage was used to scan the clinker particles after Au coating treatment. SEM and EDS-mapping pictures were got to investigate the distribution of elements in the iron-bearing mineral grains.

## 3. Results and discussion

### 3.1. Analysis of FR-CSA clinkers with different amount of CaO in raw material

#### 3.1.1. Mineralogical characterization of different FR-CSA clinkers

Fig. 1 shows the XRD patterns of the different FR-CSA clinkers. The main phases of clinkers are  $C_4A_3\bar{S}$ ,  $C_2S$ ,  $\text{CaSO}_4$ ,  $C_4AF$ , and  $C_2AS$ . The characteristic peak intensities of  $C_4AF$  and  $\text{CaSO}_4$  increase dramatically with increasing  $\text{Ca}(\text{OH})_2$ . The peaks of  $C_2AS$  are only visible in clinker  $C_{0.90}$ . Moreover, a slight d-spaces offset for the highest peak of  $C_4A_3\bar{S}$  (the cell parameter of  $C_4A_3\bar{S}$ -c and  $C_4A_3\bar{S}$ -o are (211) and (022), respectively) are observed. The d-spaces of clinkers  $C_{0.90}$ ,  $C_{0.95}$ ,  $C_{1.00}$ ,  $C_{1.05}$ , and  $C_{1.10}$  are 3.7627, 3.7621, 3.7612, 3.7596, and 3.7587 Å, respectively. With increasing CaO content in raw material, the d-spaces decrease from 3.7627 to 3.7587 Å. It is speculated that some  $\text{Fe}_2\text{O}_3$  is incorporated in  $C_4A_3\bar{S}$  mineral to form  $C_4A_{3-x}F_x\bar{S}$  in the FR-CSA clinker. The radius of  $\text{Fe}^{3+}$  ( $r = 0.069$  nm) is larger than that of  $\text{Al}^{3+}$  ( $r = 0.053$  nm) [22].  $\text{Fe}^{3+}$  occupies the octahedral position, whereas  $\text{Al}^{3+}$  occupies the tetrahedral position in the  $C_4A_{3-x}F_x\bar{S}$ . Thus, with increasing CaO content, the content of  $\text{Fe}_2\text{O}_3$  incorporated into  $C_4A_{3-x}F_x\bar{S}$  may decrease, which leads to a decrease in the volume of the unit cell structure of  $C_4A_{3-x}F_x\bar{S}$  phase and a shift of the d-space of the main peak to a smaller value.

In addition, the interplanar spacing of  $C_4A_{3-x}F_x\bar{S}$  should be increase after  $\text{Fe}_2\text{O}_3$  incorporated in  $C_4A_{3-x}F_x\bar{S}$ , but the variations of the unit cell are inconsistent in different researches. The unit cell of different FR-CSA clinkers are obtained by the Rietveld

**Table 1**  
Chemical composition in raw mixture and targeted phase compositions for FR-CSA clinkers.

	Variation	Proportions (wt.%)				
		$C_{0.90}$	$C_{0.95}$	$C_{1.00}$	$C_{1.05}$	$C_{1.10}$
FR-CSA clinker	$C_4A_3\bar{S}$	40	40	40	40	40
	$C_2S$	30	30	30	30	30
	$C_4AF$	20	20	20	20	20
	$\text{CaSO}_4$	10	10	10	10	10
	$C_m$	<b>0.90</b>	<b>0.95</b>	<b>1.00</b>	<b>1.05</b>	<b>1.10</b>
Raw material	<b>CaO</b>	<b>31.3</b>	<b>33.5</b>	<b>35.7</b>	<b>38.0</b>	<b>40.2</b>
	$\text{SiO}_2$	10.7	10.7	10.7	10.7	10.7
	$\text{CaSO}_4$	21.7	21.7	21.7	21.7	21.7
	$\text{Al}_2\text{O}_3$	24.9	24.9	24.9	24.9	24.9
	$\text{Fe}_2\text{O}_3$	6.8	6.8	6.8	6.8	6.8

**Table 2**  
Targeted phase compositions of the FR-CSA clinkers.

Targeted phases/Variation	Proportions (wt.%)									
	C <sub>0.90-1</sub>	C <sub>0.95-1</sub>	C <sub>1.00-1</sub>	C <sub>1.05-1</sub>	C <sub>1.10-1</sub>	S <sub>0</sub>	S <sub>5</sub>	S <sub>10</sub>	S <sub>15</sub>	S <sub>20</sub>
C <sub>4</sub> A <sub>3</sub> $\bar{S}$	30	30	30	30	30	50	47.5	45	42.5	40
C <sub>2</sub> S	30	30	30	30	30	30	28.5	27	25.5	24
C <sub>4</sub> AF	30	30	30	30	30	20	19	18	17	16
CaSO <sub>4</sub>	10	10	10	10	10	0	5	10	15	20
C <sub>m</sub>	<b>0.90</b>	<b>0.95</b>	<b>1.00</b>	<b>1.05</b>	<b>1.10</b>	1.00	1.00	1.00	1.00	1.00

**Table 3**  
Crystallographic structures of phases involved in the RQPA.

Phase	Space Group	ICSD code	Phase	Space Group	ICSD code
C <sub>4</sub> A <sub>3</sub> $\bar{S}$ -o	I-43m	80,361	C <sub>4</sub> A <sub>3</sub> $\bar{S}$ -c	Pcc2	9560
C <sub>2</sub> S-be	P121/n1	79,551	C <sub>2</sub> S-al'	Pnma	81,097
C <sub>4</sub> AF	Ibm2	9197	CaSO <sub>4</sub>	Bmmb	16,382
C <sub>2</sub> AS	P-421m	87,144	C <sub>5</sub> S <sub>2</sub> $\bar{S}$	Pnma	85,123
C <sub>2</sub> F	Pnma	15,059	Si	Fd-3mS	29,287

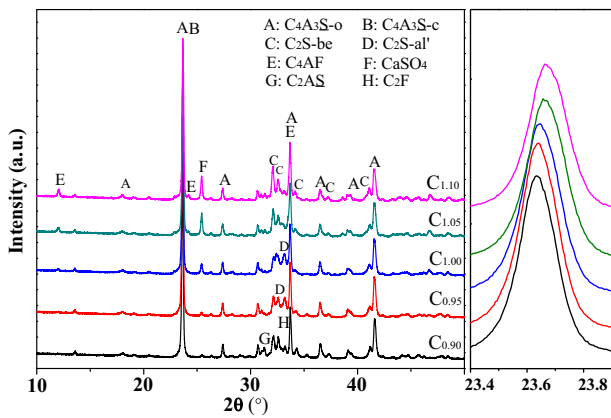


**Fig. 1.** XRD patterns of the FR-CSA clinkers with different value of C<sub>m</sub> in raw materials.

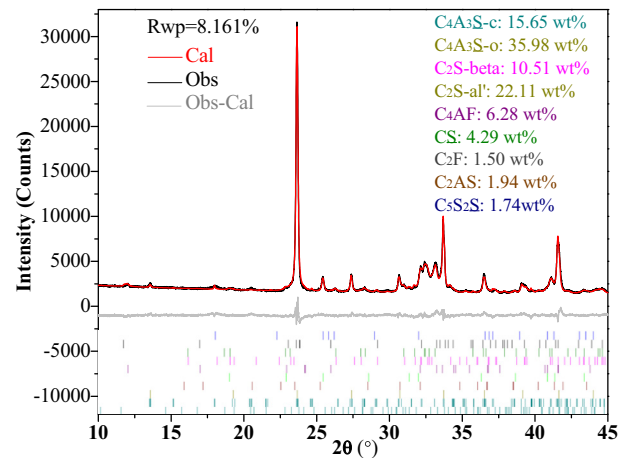


**Fig. 2.** Rietveld refinement plots of clinker C<sub>1.00</sub>. The black line indicates the experimental scan, the red line indicates the calculation pattern, the middle gray line represents the difference curve, and the short line at the bottom indicates the peak positions of different phases. (For interpretation of the references to colour in this figure legend, the reader is referred to the web version of this article.)

refinement. As shown in Table 3, the reference crystal structures are C<sub>4</sub>A<sub>3</sub> $\bar{S}$ -o and C<sub>4</sub>A<sub>3</sub> $\bar{S}$ -c. After Rietveld refinement, the unit cells of C<sub>4</sub>A<sub>3-x</sub>F<sub>x</sub> $\bar{S}$  in different FR-CSA clinkers are shown in Table 4. With the increase of CaO content in raw material, the lattice constants of cubic cell C<sub>4</sub>A<sub>3-x</sub>F<sub>x</sub> $\bar{S}$  decrease gradually. For the orthorhombic cell C<sub>4</sub>A<sub>3-x</sub>F<sub>x</sub> $\bar{S}$ , the variation of cell parameters *a* and *b* are irregular, but the parameter *c* decreases gradually. These phenomena show a good correlation with other reported results [10,15,23].

The mineral compositions of the clinkers were analyzed via RQPA using HighScore Plus software [24,25]. Fig. 2 shows the Rietveld refinement plots of clinker C<sub>1.00</sub>. The weighted profile R-factor (R<sub>wp</sub>) is 8.161%. C<sub>4</sub>A<sub>3</sub> $\bar{S}$  exists in the orthorhombic and cubic crystal structure in the clinker. C<sub>2</sub>S exists in the form of beta-C<sub>2</sub>S and alpha'-C<sub>2</sub>S. The amounts of CaSO<sub>4</sub>, C<sub>4</sub>AF, and C<sub>2</sub>F in clinker C<sub>1.00</sub>

are also calculated, as shown in Table 5. Furthermore, the amounts of different phases in clinkers C<sub>0.90</sub>, C<sub>0.95</sub>, C<sub>1.05</sub>, and C<sub>1.10</sub> are also calculated according to the RQPA results and presented in Table 5. Theoretically, the targeted phases of clinkers include C<sub>4</sub>A<sub>3</sub> $\bar{S}$ , C<sub>2</sub>S, C<sub>4</sub>AF, and CaSO<sub>4</sub>. However, the phase formation is complicate and uncontrollable in the CaO–Al<sub>2</sub>O<sub>3</sub>–Fe<sub>2</sub>O<sub>3</sub>–SO<sub>3</sub>–SiO<sub>2</sub> system [26]. Thus, small amounts of C<sub>2</sub>F, C<sub>5</sub>S<sub>2</sub> $\bar{S}$ , and C<sub>2</sub>AS are also formed in the FR-CSA clinkers, resulting in the difference between the theoretical and quantified phases. With the increase of the amount of

**Table 4**  
Refined unit cell for C<sub>4</sub>A<sub>3-x</sub>F<sub>x</sub> $\bar{S}$ .

	C <sub>4</sub> A <sub>3-x</sub> F <sub>x</sub> $\bar{S}$ -c			C <sub>4</sub> A <sub>3-x</sub> F <sub>x</sub> $\bar{S}$ -o		
	a	b	c	a	b	c
C <sub>0.90</sub>	9.210	9.210	9.210	12.957	13.001	9.220
C <sub>0.95</sub>	9.209	9.209	9.209	12.960	13.000	9.207
C <sub>1.00</sub>	9.207	9.207	9.207	13.087	13.036	9.170
C <sub>1.05</sub>	9.207	9.207	9.207	13.071	13.030	9.168
C <sub>1.10</sub>	9.204	9.204	9.204	13.068	13.029	9.162

**Table 5**

Phase compositions of different clinkers (wt.%) (Theo.: theoretical phases calculated using the Bogue equations. Quant.: phases quantified via Rietveld refinement).

Mineral	Clinkers					
	Theo.	Quant.				
		C <sub>0.90</sub>	C <sub>0.95</sub>	C <sub>1.00</sub>	C <sub>1.05</sub>	C <sub>1.10</sub>
C <sub>4</sub> A <sub>3</sub> $\bar{S}$ -o	-	14.89	16.21	15.65	16	15.23
C <sub>4</sub> A <sub>3</sub> $\bar{S}$ -c	-	40.65	37.94	35.98	31.28	28.15
<b>C<sub>4</sub>A<sub>3</sub><math>\bar{S}</math></b>	<b>40</b>	<b>55.84</b>	<b>54.15</b>	<b>51.63</b>	<b>46.98</b>	<b>43.38</b>
C <sub>2</sub> S-beta	-	25.04	17.2	10.51	11.47	27.77
C <sub>2</sub> S-alpha'	-	8.71	15.75	22.11	20.17	4.5
<b>C<sub>2</sub>S</b>	<b>30</b>	<b>33.75</b>	<b>32.95</b>	<b>32.62</b>	<b>31.64</b>	<b>32.27</b>
<b>CaSO<sub>4</sub></b>	<b>10</b>	<b>0.54</b>	<b>1.91</b>	<b>4.29</b>	<b>7.76</b>	<b>8.47</b>
C <sub>2</sub> AS	-	5.09	2.79	1.94	1.41	0.95
C <sub>5</sub> S <sub>2</sub> $\bar{S}$	-	1.16	1.79	1.74	2.41	2.99
<b>C<sub>4</sub>AF</b>	<b>20</b>	<b>2.60</b>	<b>4.93</b>	<b>6.28</b>	<b>7.92</b>	<b>9.35</b>
C <sub>2</sub> F	-	1.02	1.48	1.5	1.88	2.59

CaO in raw material, the contents of C<sub>4</sub>A<sub>3</sub> $\bar{S}$  and C<sub>2</sub>AS decrease, while the amount of C<sub>4</sub>AF, CaSO<sub>4</sub>, and C<sub>2</sub>F increases.

For the clinker C<sub>0.90</sub>, the amount of CaO is too small to exhaust Al<sub>2</sub>O<sub>3</sub>, Fe<sub>2</sub>O<sub>3</sub>, and SiO<sub>2</sub> during the calcination process. When CaO in the forms of Ca(OH)<sub>2</sub> and CaCO<sub>3</sub> are completely consumed, additional CaO from decomposing of CaSO<sub>4</sub> is required to continue to react with Al<sub>2</sub>O<sub>3</sub>, Fe<sub>2</sub>O<sub>3</sub> or SiO<sub>2</sub>, which promotes the decomposition of CaSO<sub>4</sub>. However, for the clinker C<sub>1.10</sub>, the amount of CaO is enough to react with Al<sub>2</sub>O<sub>3</sub>, Fe<sub>2</sub>O<sub>3</sub>, and SiO<sub>2</sub> according to the stoichiometric raw mixture, with only minor decomposition of CaSO<sub>4</sub>. Thus, the amount of CaSO<sub>4</sub> in FR-CSA clinker increases with increasing in CaO. In addition, although the values of C<sub>m</sub> are higher than 1.00 for clinkers C<sub>1.05</sub> and C<sub>1.10</sub>, but f-CaO does not exist in all the clinkers. Therefore, the properties of FR-CSA cement will not be influenced by f-CaO.

### 3.1.2. Incorporation levels of Fe<sub>2</sub>O<sub>3</sub> in C<sub>4</sub>A<sub>3-x</sub>F<sub>x</sub> $\bar{S}$

The experimentally quantified C<sub>4</sub>A<sub>3</sub> $\bar{S}$  content, theoretical calculated C<sub>4</sub>A<sub>3</sub> $\bar{S}$  content, and the differences between them are shown in Fig. 3. The theoretical content of C<sub>4</sub>A<sub>3</sub> $\bar{S}$  in different clinkers are 40 wt%, but the experimental results are different. With increasing amount of CaO in the raw materials, the amount determined by experiments and its deviation from theoretical amounts of C<sub>4</sub>A<sub>3</sub> $\bar{S}$  phase decrease significantly. Since the cell parameters of C<sub>4</sub>A<sub>3</sub> $\bar{S}$

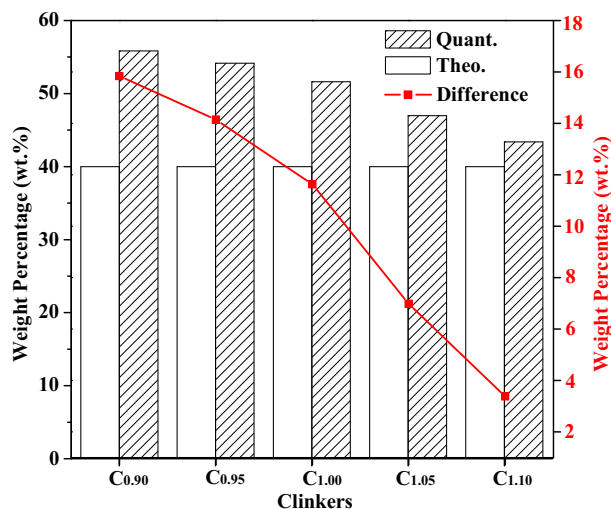


**Fig. 3.** Quantitative and theoretical amount of C<sub>4</sub>A<sub>3</sub> $\bar{S}$  and the differences between them for different FR-CSA clinkers.

and C<sub>4</sub>A<sub>3-x</sub>F<sub>x</sub> $\bar{S}$  phases are similar, the C<sub>4</sub>A<sub>3</sub> $\bar{S}$  content determined by experiments actually consists of the C<sub>4</sub>A<sub>3-x</sub>F<sub>x</sub> $\bar{S}$  and pure C<sub>4</sub>A<sub>3</sub> $\bar{S}$ . When some amount of Fe<sub>2</sub>O<sub>3</sub> are incorporated in C<sub>4</sub>A<sub>3</sub> $\bar{S}$  to form C<sub>4</sub>A<sub>3-x</sub>F<sub>x</sub> $\bar{S}$ , different incorporation levels lead to the variation of the amount of C<sub>4</sub>A<sub>3</sub> $\bar{S}$  phase determined by experiments. For the Fe<sub>2</sub>O<sub>3</sub> in the FR-CSA clinker, in addition to forming C<sub>4</sub>AF and C<sub>2</sub>F, the remaining Fe<sub>2</sub>O<sub>3</sub> replace Al<sub>2</sub>O<sub>3</sub> in C<sub>4</sub>A<sub>3-x</sub>F<sub>x</sub> $\bar{S}$ . Hence, according to previous research [27], the amount of Fe<sub>2</sub>O<sub>3</sub> involved in the substitution reaction is calculated using the Fe<sub>2</sub>O<sub>3</sub> content in C<sub>4</sub>AF and C<sub>2</sub>F. The substitution amount of Fe<sub>2</sub>O<sub>3</sub> and the values of x in C<sub>4</sub>A<sub>3-x</sub>F<sub>x</sub> $\bar{S}$  are calculated and presented in Table 6. With increasing CaO content in raw material, the incorporation levels of Fe<sub>2</sub>O<sub>3</sub> in C<sub>4</sub>A<sub>3-x</sub>F<sub>x</sub> $\bar{S}$  decrease from 17.41 wt% to 8.89 wt%. The values of x in C<sub>4</sub>A<sub>3-x</sub>F<sub>x</sub> $\bar{S}$  decrease from 0.36 to 0.18 correspondingly.

### 3.1.3. Analysis of mineral compositions by FT-IR

To verify the variation of the mineral composition among the FR-CSA clinkers, FT-IR was used to measure the chemical bonds of different phases in the FR-CSA clinkers. Infrared absorption spectra of C<sub>0.90</sub>, C<sub>0.95</sub>, C<sub>1.00</sub>, C<sub>1.05</sub>, and C<sub>1.10</sub> are shown in Fig. 4. The vibration frequencies of the clinkers are in the range of 400–1400 cm<sup>-1</sup>. As shown in Fig. 4, the absorption bands corresponding to C<sub>4</sub>A<sub>3-x</sub>F<sub>x</sub> $\bar{S}$ , CaSO<sub>4</sub>, and C<sub>2</sub>S are intense, while the bands of C<sub>2</sub>AS, C<sub>5</sub>S<sub>2</sub> $\bar{S}$ , and C<sub>2</sub>F are hardly observed due to their low content in all the clinkers. The appearance and increase in the intensities of the IR bands located at about 595 cm<sup>-1</sup> result from the vibrations of Fe–O bonds in [FeO<sub>4</sub>] tetrahedral structural units [28]. The bending vibration of the [SO<sub>4</sub>] tetrahedron in CaSO<sub>4</sub> is identified at 617 cm<sup>-1</sup> and the stretching vibration of S–O for the [SO<sub>4</sub>] groups is observed at 1156 and 1195 cm<sup>-1</sup>. The enhancement of these bands is observed in the clinkers with a C<sub>m</sub> ranging from 0.90 to 1.10, which is consistent with the results from XRD analysis. The groups of [SO<sub>4</sub>] in C<sub>4</sub>A<sub>3-x</sub>F<sub>x</sub> $\bar{S}$  are identified at 619, 663, and 987 cm<sup>-1</sup>, which are almost identical to the wavenumbers of the bands corresponding to [SO<sub>4</sub>] groups in the CaSO<sub>4</sub> [29,30]. However, the bands observed at 1100 cm<sup>-1</sup> exhibit a shift to a higher wavenumber with the addition of CaO in raw materials. This is because there

**Table 6**  
Incorporation amount of Fe<sub>2</sub>O<sub>3</sub> in C<sub>4</sub>A<sub>3-x</sub>F<sub>x</sub> $\bar{S}$ .

Clinkers	Incorporation amount (wt.%)	X
C <sub>0.90</sub>	17.72	0.36
C <sub>0.95</sub>	14.66	0.30
C <sub>1.00</sub>	13.69	0.28
C <sub>1.05</sub>	11.92	0.24
C <sub>1.10</sub>	8.96	0.18

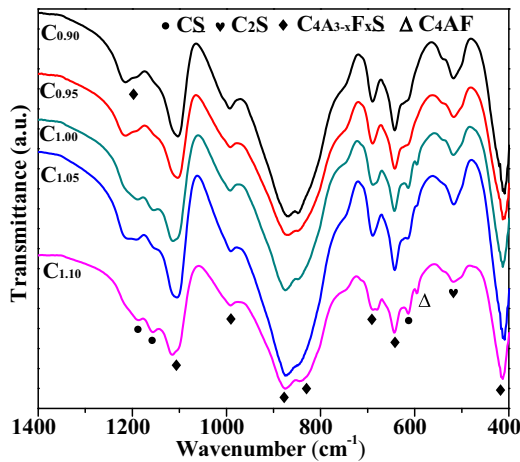


Fig. 4. FT-IR of clinkers  $C_{0.90}$ – $C_{1.10}$ .

are differences in the coordination environment of the  $[SO_4]$  group due to the incorporation of  $Fe_2O_3$  in  $C_4A_{3-x}F_x\bar{S}$ . The absorption bands located at 411, 644, 690, 821, and 875  $cm^{-1}$  are assigned to  $[AlO_4]$  groups in the  $C_4A_{3-x}F_x\bar{S}$  mineral [15,31]. With the increase of the CaO content in raw material, the band observed at 821  $cm^{-1}$  shifted to smaller wavenumber due to the decrease of Fe/Al in the  $C_4A_{3-x}F_x\bar{S}$  mineral. All of these phenomena are consistent with the results concluded by XRD analysis.

### 3.1.4. Distribution of $Fe_2O_3$ in iron-bearing minerals of the FR-CSA clinker

The SEM images of clinkers with a  $C_m$  ranging from 0.90 to 1.10 are presented in Fig. 5. The  $C_4A_{3-x}F_x\bar{S}$  exhibits a hexagonal platy structure or a quadrilateral columnar structure on the micro-level. As shown in Fig. 5, with increasing CaO content in raw material, the amount of hexagonal platy grains decreased slightly, which is consistent with the amount of  $C_4A_{3-x}F_x\bar{S}$  from XRD analysis.

To verify the proportion of  $Fe_2O_3$  in the  $C_4A_{3-x}F_x\bar{S}$ , the elemental compositions of the  $C_4A_{3-x}F_x\bar{S}$  grains are detected via SEM/EDS

analysis. Five different  $C_4A_{3-x}F_x\bar{S}$  grains in clinker  $C_{1.00}$  are selected to detect the elemental composition. The results are summarized in Fig. 6 and Table 7. The main elements (i.e., O, Ca, Al, Fe, and S) are presented in the mapping picture, and their mass fractions are listed in Table 7. The mass ratio of S:Ca:O is about 1:5:8, which is the chemical composition of  $C_4A_3\bar{S}$ . Furthermore, the total content of  $Fe_2O_3$  mixed with  $Al_2O_3$  are various in different grains, but the average  $Fe_2O_3$  content in  $C_4A_{3-x}F_x\bar{S}$  grains is approximately 14.08 wt% for clinker  $C_{1.00}$ . It is consistent with the result calculated via quantitative XRD analysis.

Similarity, another four clinkers are also tested via SEM/EDS according to this method. The results are also presented in Table 7. The incorporation levels of  $Fe_2O_3$  in  $C_4A_{3-x}F_x\bar{S}$  decrease with increasing CaO content in raw material. Furthermore, the incorporation levels of  $Fe_2O_3$  in  $C_4A_{3-x}F_x\bar{S}$  calculated by two methods are consistent. The results further demonstrate that the content of  $Fe_2O_3$  incorporated in  $C_4A_{3-x}F_x\bar{S}$  decreased with increasing CaO content in raw materials.

### 3.1.5. Effective utilization rate of $Fe_2O_3$ and $Al_2O_3$

As shown in Fig. 7, the ratios of  $Fe_2O_3$  and  $Al_2O_3$  distributed in different phases are presented respectively. With the increase of CaO content in raw material, fewer  $Fe_2O_3$  participate in the formation of  $C_4A_{3-x}F_x\bar{S}$ . Compared with the clinker  $C_{0.90}$ , about 50 wt%  $Fe_2O_3$  transfer into  $C_4AF$  and  $C_2F$  from  $C_4A_{3-x}F_x\bar{S}$  in clinker  $C_{1.10}$ . Because the hydration activity of  $C_4A_{3-x}F_x\bar{S}$  is more beneficial to the performance of the CSA cement based binders than that of  $C_4AF$  and  $C_2F$  [23], increasing CaO is not conducive to the effective utilization of  $Fe_2O_3$ . For the distribution of  $Al_2O_3$ , although the amount of  $C_4A_{3-x}F_x\bar{S}$  decreases obviously, the ratios of  $Al_2O_3$  distributed in them are almost unchanged, and all of them can reach to 90 wt%. With the increasing CaO content in raw material, the  $Al_2O_3$  content in the form of  $C_2AS$  decreases, while  $Al_2O_3$  content in the form of  $C_4AF$  increases. It is beneficial to the mechanical property development of FR-CSA cement because  $C_4AF$  has higher hydration reactivity than  $C_2AS$ . Therefore, increasing the amount of CaO in raw material can improve the effective utilization of  $Al_2O_3$ , but it inhibits  $Fe_2O_3$  incorporation in  $C_4A_{3-x}F_x\bar{S}$ .

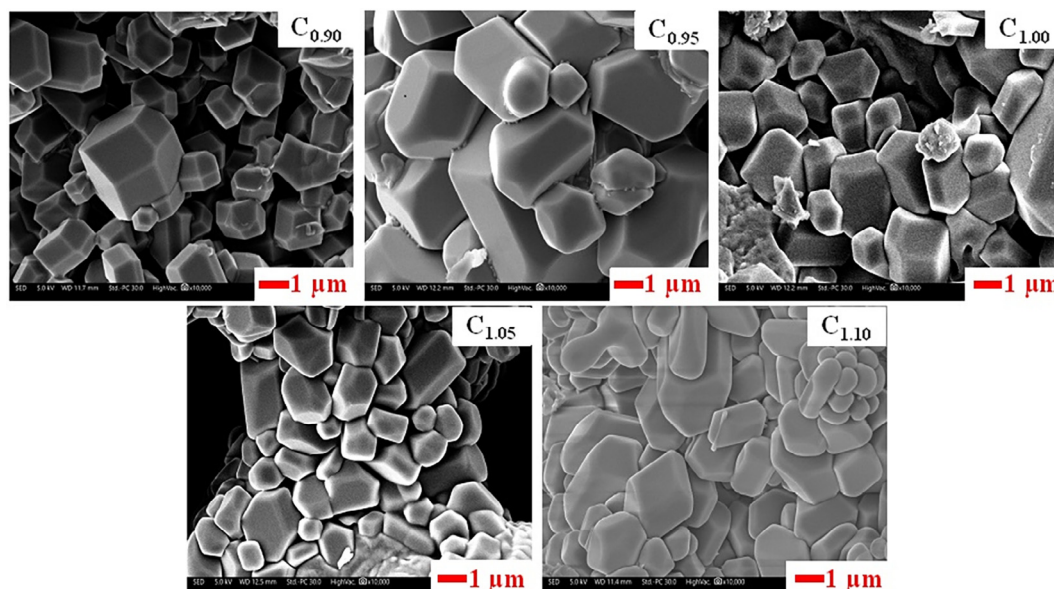


Fig. 5. SEM images of clinkers  $C_{0.90}$ – $C_{1.10}$ .

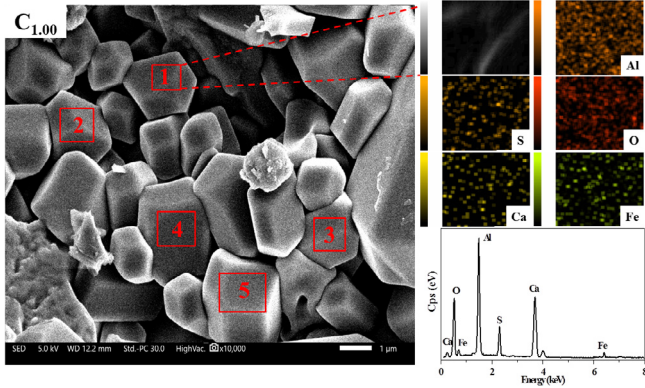


Fig. 6. SEM/EDS image and elemental composition map of clinker C<sub>1.00</sub>.

3.2. Effect of CaO content on iron-bearing phase composition of FR-CSA clinker with 30 wt% C<sub>4</sub>AF

The effect of CaO on the phase composition of FR-CSA clinker is investigated based on FR-CSA clinker with 30 wt% C<sub>4</sub>AF. The XRD patterns of these clinkers are shown in Fig. 8. The types of minerals in clinkers are almost the same with those in the FR-CSA clinker with 20 wt% C<sub>4</sub>AF. For the FR-CSA clinker with 30 wt% C<sub>4</sub>AF and a C<sub>m</sub> of 0.90, the XRD peaks of CaSO<sub>4</sub> are detected. The characteristic peaks of C<sub>2</sub>AS don't exist in the FR-CSA clinker. More importantly, with increasing CaO content in raw materials, the C<sub>4</sub>AF content increases clearly and the main characteristic peak of

C<sub>4</sub>A<sub>3-x</sub>F<sub>x</sub>S̄ also shifts to higher angles. It conclude that the incorporation content of Fe<sub>2</sub>O<sub>3</sub> in C<sub>4</sub>A<sub>3-x</sub>F<sub>x</sub>S̄ also decrease with increasing of CaO content in raw material, which is consistent with the phenomenon that 20 wt% C<sub>4</sub>AF is designed in the FR-CSA clinker.

Thus, during the calcination process of FR-CSA clinker, the CaO content in raw material influence the phase composition of clinker. With the increase of CaO content, the incorporation level of Fe<sub>2</sub>O<sub>3</sub> in C<sub>4</sub>A<sub>3-x</sub>F<sub>x</sub>S̄ decreases, which led to more C<sub>4</sub>AF and fewer C<sub>4</sub>A<sub>3-x</sub>F<sub>x</sub>S̄ formed.

3.3. Effect of CaO in the form of CaSO<sub>4</sub> on iron-bearing phase formation of FR-CSA clinker

Fig. 9 presents the XRD patterns of FR-CSA clinkers designed with different extra amounts of CaSO<sub>4</sub>, respectively. It demonstrates that a part of CaO in the form of CaSO<sub>4</sub> doesn't react with other materials during the calcination process. In the proportion design of the raw mixture, all of CaO in the form of CaSO<sub>4</sub> are used to calculate the value of C<sub>m</sub>. However, CaSO<sub>4</sub> doesn't fully decompose for the clinkers with the extra amount of CaSO<sub>4</sub> more than 5 wt%. Thus the C<sub>m</sub> values are actually less than 1.00. Moreover, when the extra amount of CaSO<sub>4</sub> of clinkers increases from 0 to 20 wt%, the amount of undecomposed CaSO<sub>4</sub> also increases. That is to say, the amount of CaO involved in the calcination reaction decreases, which restricts the reaction of C<sub>2</sub>AS consumption according to Eq. (5), the amount of C<sub>2</sub>AS increases in FR-CSA clinkers.

In addition, with increasing extra CaSO<sub>4</sub> content in raw materials, the C<sub>4</sub>AF content in clinkers decreases, while the differences

Table 7  
Chemical composition of areas in the C<sub>4</sub>A<sub>3-x</sub>F<sub>x</sub>S̄ grains (wt.%).

Clinkers	Areas	O	Ca	Al	Fe	S	W(Fe <sub>2</sub> O <sub>3</sub> )/W(Al <sub>2</sub> O <sub>3</sub> + Fe <sub>2</sub> O <sub>3</sub> )
C <sub>1.00</sub>	1	41.73	24.03	22.38	4.47	5.23	13.12
	2	42.08	24.83	19.93	5.29	5.46	16.71
	3	42.34	24.14	21.86	4.14	5.27	12.52
	4	41.94	22.66	22.31	5.04	5.92	14.59
	5	42.49	24.68	21.63	4.43	5.18	13.41
C <sub>0.90</sub>	Average	42.21	24.30	20.40	5.55	5.32	17.06
C <sub>0.95</sub>	Average	42.39	24.16	20.96	4.64	5.69	14.34
C <sub>1.00</sub>	Average	42.11	24.06	21.62	4.67	5.42	14.04
C <sub>1.05</sub>	Average	43.44	23.88	21.94	3.88	5.53	11.79
C <sub>1.10</sub>	Average	43.66	22.95	22.14	3.14	6.18	9.68

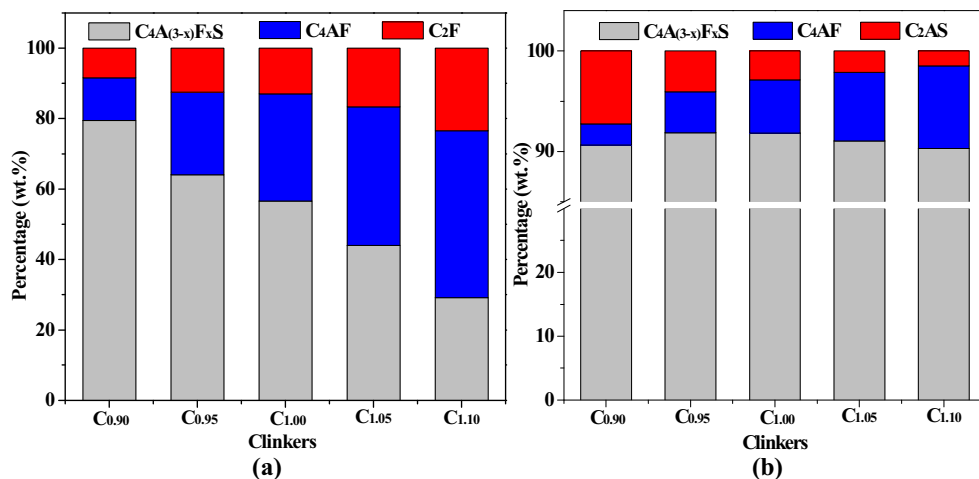


Fig. 7. Ratios of Fe<sub>2</sub>O<sub>3</sub> and Al<sub>2</sub>O<sub>3</sub> distributed in different minerals (a: Fe<sub>2</sub>O<sub>3</sub>, b: Al<sub>2</sub>O<sub>3</sub>).

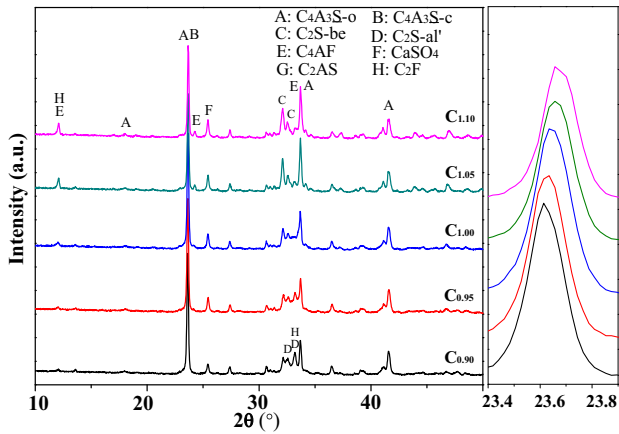


Fig. 8. XRD patterns of the FR-CSA clinkers with 30 wt%  $C_4AF$  content designed.

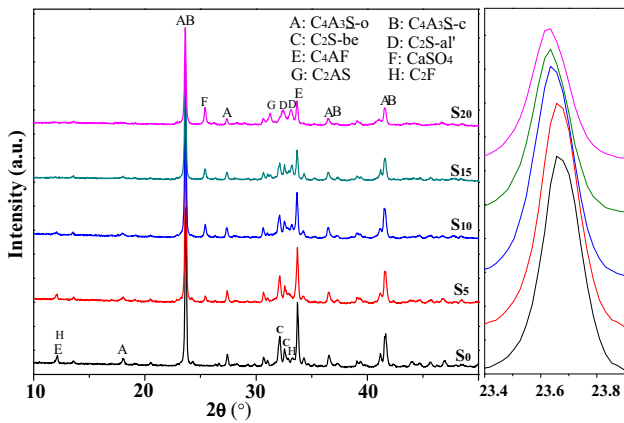


Fig. 9. XRD patterns of the FR-CSA clinkers with different  $CaSO_4$  content in raw materials.

between the theoretically calculated and experimentally determined content of  $C_4A_{3-x}F_x\bar{S}$  increase. Meanwhile, the highest peak of  $C_4A_{3-x}F_x\bar{S}$  also shifts to lower angles according to their XRD patterns and the d-spaces of them increase from 3.7520 to 3.7614 Å. It

demonstrates that the volume of the unit cell structure of  $C_4A_{3-x}F_x\bar{S}$  increases. Thus, according to the change of unit cell structure and the variation of mineral composition, it is concluded that the content of  $Fe_2O_3$  incorporated in  $C_4A_{3-x}F_x\bar{S}$  increases with increasing extra  $CaSO_4$  content in raw material

In a word, with increasing extra  $CaSO_4$  content in raw materials, the  $CaO$  content involved in chemical reaction during calcination process decreases, leading to the increase of  $Fe_2O_3$  content incorporated in  $C_4A_{3-x}F_x\bar{S}$ . It is consistent with the variation caused by changes in  $CaO$  content.

### 3.4. Effect of $CaO$ content variation caused by calcination temperature and holding time on the iron-bearing phase formation of FR-CSA clinker

Calcination temperature and holding time during calcination process of the FR-CSA clinker not only affect the formation of reactive minerals but also can affect the decomposition of  $CaSO_4$ . Thus the effects of calcination temperature and holding time on the iron-bearing phase composition of the FR-CSA clinker were also investigated. The XRD results are shown in Fig. 10.

With the increase of calcination temperature, the intensity of  $CaSO_4$  diffraction peaks decrease and disappear finally. It means that more  $CaSO_4$  were decomposed, resulting in that more  $CaO$  participate in the mineral formation during the calcination process. Meanwhile, the intensity of  $C_4AF$  diffraction peaks increases, while the intensity of  $C_4A_{3-x}F_x\bar{S}$  decreases. It demonstrates that the content of  $Fe_2O_3$  incorporated in the  $C_4A_{3-x}F_x\bar{S}$  decreases with the increase in calcination temperature. Similarly, as shown in Fig. 10(b), with the increase in holding time, the intensity of  $CaSO_4$  diffraction peaks decrease and those of  $C_4AF$  increase. It is consistent with the phenomenon caused by the changing of calcination temperature. Increasing the calcination temperature and holding time cause more  $CaO$  to participate in the mineral formation reaction, accompanied by an increase in  $C_4AF$  content and a decrease in  $C_4A_{3-x}F_x\bar{S}$  content, which further demonstrates that more  $CaO$  content involved in the reaction can make less  $Fe_2O_3$  incorporated in  $C_4A_{3-x}F_x\bar{S}$ . Therefore, when the calcination temperature is between 1200 °C and 1300 °C, the effects of calcination temperature and holding time on the iron-bearing phase composition are mainly caused by their influence on the decomposition degree of  $CaSO_4$  and the content of  $CaO$  involved in mineral formation reactions.

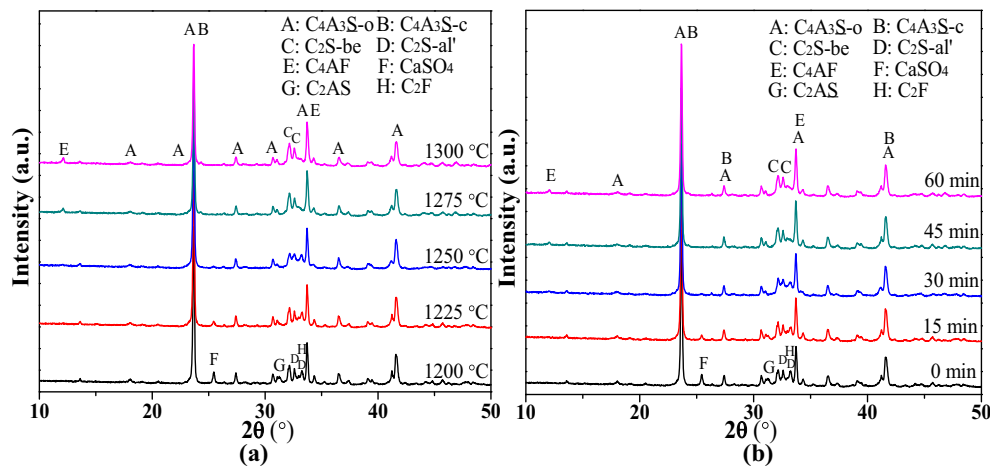


Fig. 10. XRD patterns of the FR-CSA clinkers with different calcination temperature and maintained time (a: Different temperature, b: Different holding time).

## 4. Conclusion

This research demonstrated the effect of CaO content in raw material on iron-bearing phase composition of FR-CSA clinker. The CaO content in raw material significantly influences the phase formation in the FR-CSA clinker during the calcination process, especially for the formation of iron-bearing phases.

With the reduction of CaO content in the form of  $\text{CaCO}_3$  or  $\text{Ca}(\text{OH})_2$  in raw materials, the amount of  $\text{C}_4\text{AF}$  formed in the FR-CSA clinkers decreased and the amount of  $\text{Fe}_2\text{O}_3$  incorporated in  $\text{C}_4\text{A}_{3-x}\text{F}_x\bar{\text{S}}$  increased. When the  $C_m$  is 0.90 and 20 wt%  $\text{C}_4\text{AF}$  are designed in the FR-CSA clinker, the value of  $x$  in the  $\text{C}_4\text{A}_{3-x}\text{F}_x\bar{\text{S}}$  can be up to 0.36.

For the CaO content existed in the form of  $\text{CaSO}_4$  in raw material, it presents a similar effect. When the CaO content is constant and the  $\text{CaSO}_4$  content increases in raw material, the CaO content involved in the calcination reaction decreased, which also lead to an increase in the amount of  $\text{Fe}_2\text{O}_3$  incorporated in  $\text{C}_4\text{A}_{3-x}\text{F}_x\bar{\text{S}}$ .

The findings in this study make it possible to optimize the mineral composition of the FR-CSA clinker by changing the CaO content in the raw materials. Furthermore, low CaO content in raw material is beneficial to the formation of  $\text{C}_4\text{A}_{3-x}\text{F}_x\bar{\text{S}}$ , which enables that some solid wastes containing low calcium or low aluminum can also be used as raw materials for FR-CSA cement production.

## CRedit authorship contribution statement

**Xingliang Yao:** Methodology, Formal analysis. **Shizhao Yang:** Formal analysis, Investigation. **Hua Dong:** Data curation. **Shuang Wu:** Validation. **Xuhui Liang:** Data curation. **Wenlong Wang:** Conceptualization, Resources, Project administration.

## Declaration of Competing Interest

The authors declare that they have no known competing financial interests or personal relationships that could have appeared to influence the work reported in this paper.

## Acknowledgments

The authors acknowledge the support of the National Key Research & Development Program of China (No. 2017YFC0703100), Shandong Provincial Major Scientific and Technological Innovation Project (No. 2019JZZY020306). This research is also funded by the China Scholarship Council.

## References

- [1] L. Zhang, M.Z. Su, Y.M. Wang, Development of the use of sulfo- and ferroaluminate cements in China, *Adv. Cement Res.* 11 (1) (1999) 15–21.
- [2] F.P. Glasser, L. Zhang, High-performance cement matrices based on calcium sulfoaluminate-belite compositions, *Cement Concr. Res.* 31 (12) (2001) 1881–1886.
- [3] M. Chen, B. Liu, L. Li, L. Cao, Y. Huang, S. Wang, et al., Rheological parameters, thixotropy and creep of 3D-printed calcium sulfoaluminate cement composites modified by bentonite, *Compos. Part B: Eng.* (2020) 107821.
- [4] I.A. Chen, M.C.G. Juenger, Synthesis and hydration of calcium sulfoaluminate-belite cements with varied phase compositions, *J. Mater. Sci.* 46 (8) (2010) 2568–2577.
- [5] C. Liu, J. Luo, Q. Li, S. Gao, D. Su, J. Zhang, et al., Calcination of green high-belite sulfoaluminate cement (GHSC) and performance optimizations of GHSC-based foamed concrete, *Mater. Des.* 182 (2019) 107986.
- [6] T. Hanein, J.-L. Galvez-Martos, M.N. Bannerman, Carbon footprint of calcium sulfoaluminate clinker production, *J. Cleaner Prod.* 172 (2018) 2278–2287.
- [7] C.W. Hargis, A.P. Kirchheim, P.J.M. Monteiro, E.M. Gartner, Early age hydration of calcium sulfoaluminate (synthetic ye'elimite,) in the presence of gypsum and varying amounts of calcium hydroxide, *Cem. Concr. Res.* 48 (2013) 105–115.
- [8] V. Morin, P. Termkhajornkit, B. Huet, G. Pham, Impact of quantity of anhydrite, water to binder ratio, fineness on kinetics and phase assemblage of belite-ye'elimite-ferrite cement, *Cement Concr. Res.* 99 (2017) 8–17.
- [9] Y.M. Wang, M. Su, L. Zhang, Sulphoaluminate Cement, Press Beijing Univ.
- [10] D. Chen, X.J. Feng, S.Z. Long, The influence of ferric oxide on the properties of  $3\text{CaO}\cdot3\text{Al}_2\text{O}_3\cdot\text{CaSO}_4$ , *Thermochimica Acta.* 215 (1993) 157–169.
- [11] G. Möschner, B. Lothenbach, F. Winnefeld, A. Ulrich, R. Figi, R. Kretzschmar, Solid solution between Al-ettringite and Fe-ettringite ( $\text{Ca}_6[\text{Al}_{1-x}\text{Fe}_x(\text{OH})_6]_2(\text{SO}_4)_3\cdot26\text{H}_2\text{O}$ ), *Cem. Concr. Res.* 39 (6) (2009) 482–489.
- [12] D. Ectors, J. Neubauer, F. Goetz-Neunhoeffer, The hydration of synthetic brownmillerite in presence of low Ca-sulfate content and calcite monitored by quantitative in-situ-XRD and heat flow calorimetry, *Cem. Concr. Res.* 54 (2013) 61–68.
- [13] A. Cuesta, I. Santacruz, S.G. Sanf elix, F. Fauth, M.A.G. Aranda, A.G. De la Torre, Hydration of C4AF in the presence of other phases: a synchrotron X-ray powder diffraction study, *Constr. Build. Mater.* 101 (2015) 818–827.
- [14] Y. Huang, X.D. Shen, S.H. Ma, L. Chen, Q. ZB, Effect of  $\text{Fe}_2\text{O}_3$  on the formation of calcium sulfoaluminate mineral, *J. Chinese Ceram. Soc.* 35 (4) (2005) 485–489.
- [15] M. Idrissi, A. Diouri, D. Damidot, J.M. Grenèche, M.A. Talbi, M. Taibi, Characterisation of iron inclusion during the formation of calcium sulfoaluminate phase, *Cem. Concr. Res.* 40 (8) (2010) 1314–1319.
- [16] B. Touzo, K.L. Scrivener, F.P. Glasser, Phase compositions and equilibria in the  $\text{CaO}\text{--}\text{Al}_2\text{O}_3\text{--}\text{Fe}_2\text{O}_3\text{--}\text{SO}_3$  system, for assemblages containing ye'elimite and ferrite  $\text{Ca}_2(\text{Al}, \text{Fe})\text{O}_5$ , *Cem. Concr. Res.* 54 (2013) 77–86.
- [17] A. Berrio, C. Rodr guez, J.I. Tob n, Effect of  $\text{Al}_2\text{O}_3/\text{SiO}_2$  ratio on ye'elimite production on CSA cement, *Constr. Build. Mater.* 168 (2018) 512–521.
- [18] C. Ren, W. Wang, G. Li, Preparation of high-performance cementitious materials from industrial solid waste, *Constr. Build. Mater.* 152 (2017) 39–47.
- [19] Y. Shen, J. Qian, Y. Huang, D. Yang, Synthesis of belite sulfoaluminate-ternesite cements with phosphogypsum, *Cem. Concr. Compos.* 63 (2015) 67–75.
- [20] X. Yao, W. Wang, M. Liu, Y. Yao, S. Wu, Synergistic use of industrial solid waste mixtures to prepare ready-to-use lightweight porous concrete, *J. Cleaner Prod.* 211 (2019) 1034–1043.
- [21] S. Wu, W. Wang, C. Ren, X. Yao, Y. Yao, Q. Zhang, et al., Calcination of calcium sulfoaluminate cement using flue gas desulfurization gypsum as whole calcium oxide source, *Constr. Build. Mater.* 228 (2019) 116676.
- [22] O. Andac PPG, Polymorphism of calcium sulfoaluminate ( $\text{Ca}_4\text{A}160\text{16}\bullet\text{S03}$ ) and its solid solutions, *Adv. Cement Res.* 22 (6) (1994) 57–60.
- [23] F. Bullerjahn, D. Schmitt, M. Ben Haha, Effect of raw mix design and of clinkering process on the formation and mineralogical composition of (ternesite) belite calcium sulfoaluminate ferrite clinker, *Cem. Concr. Res.* 59 (2014) 87–95.
- [24] G.  lvarez-Pinazo, A. Cuesta, M. Garc a-Mat e, I. Santacruz, E.R. Losilla, A.G.D. la Torre, et al., Rietveld quantitative phase analysis of Yeelimite-containing cements, *Cem. Concr. Res.* 42 (7) (2012) 960–971.
- [25] A.J. Cuberos, A.G. De la Torre, G.  lvarez-Pinazo, M.C. Martin-Sedeno, K. Schollbach, H. Pollmann, et al., Active iron-rich belite sulfoaluminate cements: clinkering and hydration, *Environ. Sci. Technol.* 44 (17) (2010) 6855–6862.
- [26] S. Sahu, J. Majling, Phase compatibility in the system  $\text{CaO}\text{--}\text{SiO}_2\text{--}\text{Al}_2\text{O}_3\text{--}\text{Fe}_2\text{O}_3\text{--}\text{SO}_3$  referred to sulfoaluminate belite cement clinker, *Cem. Concr. Res.* 23 (6) (1993) 1331–1339.
- [27] X. Yao, S. Yang, Y. Huang, S. Wu, Y. Yao, W. Wang, Effect of  $\text{CaSO}_4$  batching in raw material on the iron-bearing mineral transition of ferric-rich sulfoaluminate cement, *Constr. Build. Mater.* 250 (2020) 118783.
- [28] S. Rada, A. Dehelean, E. Culea, FTIR, Raman, and UV-Vis spectroscopic and DFT investigations of the structure of iron-lead-tellurate glasses, *J. Mol. Model.* 17 (8) (2011) 2103–2111.
- [29] M. Montes, E. Pato, P.M. Carmona-Quiroga, M.T. Blanco-Varela, Can calcium aluminates activate ternesite hydration?, *Cem. Concr. Res.* 103 (2018) 204–215.
- [30] P. Julphunthong, Synthesizing of calcium sulfoaluminate-belite (CSAB) cements from industrial waste materials, *Mater. Today: Proc.* 5 (7) (2018) 14933–14938.
- [31] Y. Guo, J. Deng, M. Su, Y. Wang, A study on formation mechanism of ferrite phase in ferroaluminate cement, *J. Chinese Ceram. Soc.* 16 (6) (1988) 481–488.